ELSEVIER

Surface and Coatings Technology 131 (2000) 109–115

SURFACE & COATINGS TECHNOLOGY

www.elsevier.nl/locate/surfcoat

Plasma surface engineering in first wall of tokamak

Zhen Kui Shang, Zeng Yu Xu*, Xi Wen Deng, Xiang Liu, Nian Man Zhang

Southwestern Institute of Physics, P.O. Box 432, Chengdu, 610041 Sichuan, PR China

Abstract

Plasma facing wall condition is very important for the energy confinement of plasma in a tokamak machine. The boronization, siliconization and lithium coating of the inner wall of HL-1M are introduced here, and the hydrogen recycling and influence on controlled impurities and core radiation energy loss are discussed. Experiments show that these wall treatments are very useful for plasma confinement; a 4-s reproducible long pulse discharge is obtained for siliconized wall, but the plasma pulse length only achieves 2.1 s and its reproducibility is very poor for boronized wall. Lithium coating is the best method of wall treatment for lowering hydrogen recycling and decreasing the impurities level. For the applications of HL-2A and the future fusion device, a series of B, Ti, Si-doped graphite and B_4C–C/C composites have been developed, some experimental results for chemical sputtering, tritium retention and recycling, as well as high heat loads are reviewed. Meanwhile, SiC, TiC and B_4C coating, and B_4C–C, SiC–C, B_4C–Cu, Mo–Cu and W–Cu functionally graded materials are also introduced.

Keywords: First wall; Wall treatment; Plasma-facing material

1. Introduction

Tokamak is the major controlled nuclear fusion device; the design and construction of the first wall of tokamak is one of utmost importance. The inner wall of a tokamak machine consists of plasma facing materials, such as graphite, C/C composite and beryllium, and structural materials, such as 316 stainless steel and ferrite steel. Up to now, graphite was most widely used for plasma facing material. For the special parts of the first wall, such as the divertor and limiter, high heat flux components must be adopted because much higher thermal load will occur at these positions; therefore, high-strength, high-melting point materials are always preferential. Research of high heat flux components tends to focus on SiC, TiC, and B_4C coatings and W–Cu and Mo–Cu mixtures.

In HL-1M tokamak, the first wall is 316 ss, with only 6% area covered by graphite blocks. During glow discharge, a lot of carbon impurity and heavy metal impurities will be released into the plasma, which will induce the loss of plasma energy and influence the properties of plasma confinement. Therefore, some wall treatments are necessary. In this paper, the boronization, siliconization and lithium coating of the inner wall of HL-1M are introduced, and their influences on tokamak plasma are discussed.

Mentioned above, boronization, siliconization and lithium coating of the inner wall can effectively improve the properties of plasma confinement; the modification of carbon materials was also carried out. In recent years, B, Ti, Si-doped graphite and B_4C–C/C composites have been developed, and experimental results show that they are superior to high purity graphite on restraining chemical sputtering, decreasing tritium retention and recycling, and resisting thermal shock. In this paper, the properties of B, Ti, Si-doped graphite are reviewed; and some experimental results both in

* Corresponding author. Tel.: +86-285-581122; fax: +86-285-581458.

E-mail address: xuzy@swip.edu.cn (Z. Yu Xu).

0257-8972/00/$ - see front matter
PII: S0257-8972(00)00819-7

modified facility and HL-1M tokamak machine are obtained. In addition some high heat flux components materials, such as SiC and TiC coatings and B_4C–C, B_4C–Cu, Mo–Cu and W–Cu functionally graded materials (FGM) are discussed.

2. The wall coating of HL-1M

2.1. Boronization

The inner wall of the vacuum chamber of HL-1M consists of stainless steel with only 6% area covered by graphite blocks. When HL-1M operates with high parameters, $B_T = 3$T, $I_p = 300$ kA and 2 MW high power auxiliary heating, impurity control and a low hydrogen recycling of the inner wall are needed. One way to resolve the problem is wall treating by boronization, siliconization and lithium coating [1–3].

The boronization is carried out in a He glow discharge with $C_2B_{10}H_{12}$ addition. Operating conditions are as follows [4]: DC current is 1.0–1.5 A with a single electrode. DC voltage is 800–1000 V. Pressure is 10^{-3}–10^{-4} Torr. Ratio of $C_2B_{10}H_{12}$ vapor to He pressure is 0.1:1.0. Temperature of vacuum vessels of the boronization system is 80–100°C. Deposition time is approximtely 1 h.

After the boronization of the inner wall, a-B/C:H film was formed on the wall surface, the thickness of the coating is 50–70 nm and the ratio of boron to carbon is 1:6.

2.2. Siliconization [4,5]

The process is similar to boronization and uses DC glow discharge with a mixture of 5–10% SiH_4 and 95–90% He. The thickness of a C/Si:H film is about 100 nm, and major components in the coating are Si, C and SiC by means of X-ray Photoelectron Spectroscopy (XPS) analysis.

2.3. Lithium coating [4,5]

Lithium is deposited on the inner wall of HL-1M by plasma-assisted deposition, a few blocks of solid lithium weighing 2 g are put in an oven under Ar gas flow to prevent the lithium from oxidation, and the oven can be moved radially inwards and outwards. Solid lithium blocks were heated up to 600°C, evaporated into a He glow discharge where they ionized and finally deposited on the wall as the discharge cathode. The discharge pressure ($P_{H2} + P_{li}$) is 35×10^{-2} Pa and the current density is 10–12 $\mu A/cm^2$ with 400–500-V anode voltage. The deposition runs for about 10 min at room temperature, and approximately 1 g of lithium is deposited on the wall; the average film thickness is estimated at approximately 10 nm.

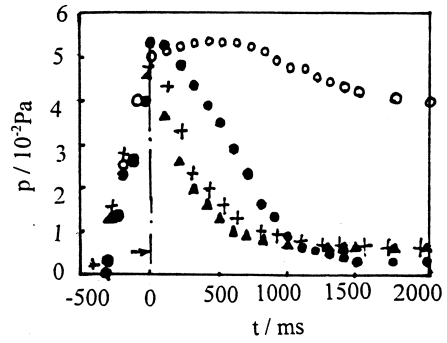

Fig. 1. Neutral gas pressure changing with time in SOL layer after different wall surface treatment: $t = 0$, discharge is beginning; (O), no discharge; (●), boronization; (+), siliconization; (▲), lithium coating.

2.4. Hydrogen retention and recycling

Fig. 1 shows the neutral gas pressure changing with time in the scrape-off layer after different wall conditioning during tokamak discharge; it shows hydrogen recycling performance in the edge plasma. From Fig. 1 it can be seen that hydrogen recycling of boronized wall is obviously higher than that of siliconized wall and lithium coating, and hydrogen recycling of siliconized wall is a little higher than that of the lithium coated wall. When the additional hydrogen gas is pumped in, the phenomenon above can be observed more clearly.

In order to test the absorption ability of the wall surface to hydrogen by different wall treating without discharge, equal amounts of hydrogen gas ($P_{H2} = 5.3 \times 10^{-2}$ Pa, $\Delta t = 30$ ms) were pumped into the vacuum chamber just after every wall treatment, and the gas compositions in the vacuum chamber were measured by QMS (shown in Fig. 2). As can be seen from Fig. 2, a-C/Si:H film, lithium coating is inert for hydrogen

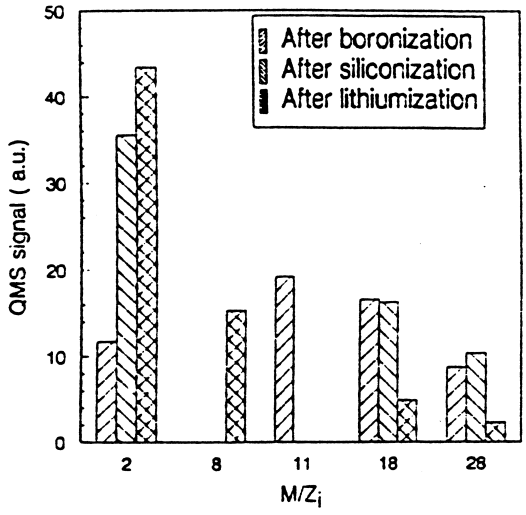

Fig. 2. QMS signal in main chamber during pulse blow gas after different wall surface treatment.

molecules, but B/C film has a strong absorption capacity, which is regarded as physical absorption. For siliconized and lithiumized wall, no chemical reaction occurred between Si, Li and H_2 at room temperature, That is why hydrogen recycling during a tokamak discharge from boronized wall is higher than that from siliconized or lithiumized wall. Another reason for the lower hydrogen recycling by siliconization and lithium coating treating is the strong chemical affinity of silicon and lithium for hydrogen ions or atoms. In fact, during a tokamak discharge, the strong pumped effect to hydrogen has been observed for siliconiztion and lithium coating wall treating [4,5].

2.5. The influence on tokamak discharge of different wall treating

Because the boronization materials contain some qualities of carbon, when tokamak discharge occurred, the boron atoms in B/C film are preferential sputtering, unstable wall conditions appear after several boronization cycles. As a result, the wall outgassing and impurity intensity sharply increase, leading to disruptive shots when pellets are injected in the pellets fueling experiment or in the LHCD experiment. In the long pulse discharge experiments, only 2.1-s plasma pulse length was achieved and its reproducibility is very poor. But the wall conditions stay stable over a long time and the wall gassing and impurity are controlled effectively by siliconization. In the pellet-fueling experiments, almost no disruption shots occur. The driving power in the LHCD experiments rise to 850 kW and the reproducible long pulse discharges with 4-s plasma pulse length are obtained (as seen in Fig. 3).

The primary discharge experiment by lithium coating demonstrates its superiorioity. Fig. 4 shows the core radiation power loss in the first shot after the different wall treating under the same discharge parameters. From Fig. 4, it can be seen that the core radiation power loss reduces to the lowest level with a fresh lithium coating, but the superiority lasts only several

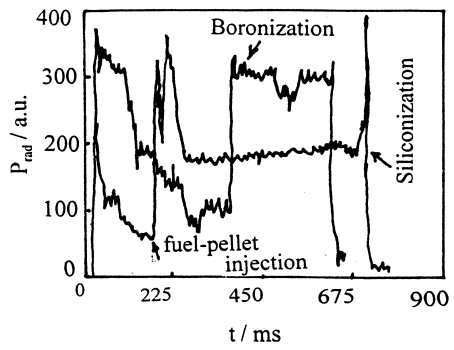

Fig. 3. Plasma core heat radiation loss after fuel-pellet injection in different wall conditions.

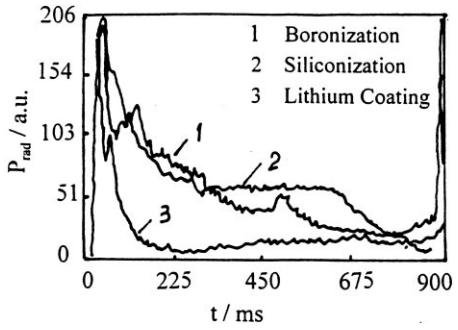

Fig. 4. Plasma core heat radiation loss in the first shot after different wall surface treatment.

shots, which indicates that to prolong the lifetime of lithium coating is a problem to be resolved.

3. Plasma facing materials

3.1. B, Ti, Si-doped graphite and B_4C–C/C composites

A series of B, Ti, Si-doped graphite have been developed by hot pressing; the average density is ~2–2.17 g/cm^3, which is close to the limited graphite density 2.26 g/cm^3. The porosity of B, Ti, Si-doped graphite is lower than that of high purity graphite. The bend strength of B, Ti, Si-doped graphite is higher than that of high purity graphite by 2–3 times, and the thermal conductivity of the doped graphite is a little lower than that of high purity graphite. The physical and thermomechanical properties are listed in Table 1. The concentration of boron, titanium or silicon is 3–20%, respectively. Microstructure analysis reveals that only about 2% B, Ti or Si can be dissolved in the graphite matrix while the additional amounts exist with compounds, such B_4C, SiC or TiB_2.

Three-dimensional C/C composites are made by means of hot isostatic press; its average density is 1.94 g/cm^3 and the porosity is about 3–6%. The concentration of boron in B_4C–C/C composites is 3–7 wt.%, the physical properties of C/C composites are shown in Table 2. The thermal conductivity of C/C (4#) is close to the level of C/C composites abroad and is homogeneous.

3.2. Chemical sputtering [6]

When the B, Ti, Si-doped graphite was bombarded by deuterium ions with 1 keV energy at elevated temperature, the methane yield was measured by QMS. The experimental results are shown in Fig. 5. From Fig. 5, it can be seen that the methane yields CD_4 of the doped graphite are much lower than that of high purity graphite TPMS and the peak temperatures of CD_4 for the doped graphite moved towards the lower temperature with the increase in boron. Comparing with the experimental results of chemical sputtering for RG–Ti,

Table 1
Physical properties of some doped graphite

Material types	Content of dopants (wt. %)	Density (g/cm^3)	Porosity (%)	Bend strength (MPa)	Thermal expansion coefficient ($10^{-6}/K$)	Thermal conduct (W/m.K)
TPMS	–	1.83	< 10	34.2	2.95	72.0
TPMSBS-10	B 10% + Si 5%	2.10	4.70	102.9	3.06	39.6
TPMSBST-8–6	B 8 + Ti 6 + Si 4	2.17	4.93	123.3	2.96	59.4
TPMSBST-9–4	B 9 + Ti 4.8 + Si1.6	2.12	5.33	123.2	2.95	68.4
GB110	B 10	2.00	6.14	81.1		48.6
GBT78	B 7 + Ti 8	2.13	5.7	74.3	3.38	71.7
GBT155	B 15 + Ti 5	2.12	5.23	90.9		75.3
GBT205	B 20 + Ti 5	2.09	6.34	104.1	4.78	71.25
GTB10610	B 10 + Ti 6	2.18	4.18	67		48.6
GBS33	B 3 + Si 3	2.0	6.5			100.4
RG–Ti	Made by Russia	2.20				400
USB15	Made by Russia	1.8	12.0			100

RG–Ti–B and USB15 made by Russia, chemical sputtering yields of B, Ti, Si-doped graphite made by China are lower than that of RG–Ti and RG–Ti–B and slightly higher than that of USB15.

3.3. Hydrogen retention and recycling

As mentioned above, some amounts of boron increased in graphite can effectively reduce the chemical sputtering yields; it is believed that hydrogen retention and recycling of B, Ti, Si-doped graphite should be decreased as well. A thermal desorption experiment was carried out, and the TDS of GB110 graphite (10 wt.%B), high purity graphite ISO880U and B_4C coating on copper were measured (Fig. 6). The peak temperature of methane obviously moved to the lower temperature direction for GB110 and B_4C coating. The mechanism of thermal desorption of methane in boron-doped graphite was investigated. There are three process that contribute to methane release in boron-doped graphite [7]: (1) methane forms at the internal pore surface and freely diffuses through the internal channels; (2) methane forms by the chemical reaction between the hydrogen atoms trapped in B_4C precipitates and the carbon atoms from B_4C compounds; and (3) methane forms in the matrix lattices and desorbs by bulk diffusion.

3.4. Thermal shock

In the future fusion reactor, one of the functions of plasma facing materials is to remove the thermal deposition from plasma; therefore, high heat load on the plasma-facing materials is the most important issue. In the past 10 years, the experimental facilities of high heat load were constructed and thermal shock tests were carried out with pulse laser and electron beam [8,9]. According to a simple plate-shaped model [10], fracture failure will occur when the surface temperature just exceeds the minimum critical value $\Delta T_c = \sigma_F (1-\nu)/S\alpha E$, where σ_F denotes the critical stress associated with the fracture failure mode, ν is Poisson's ratio, α is the linear thermal expansion coefficient, E is Young's modulus, $\Delta T_c = T - T_0$ is the surface tem-

Table 2
Physical properties of C/C composites

Material types	Composition	Density (g/cm^3)	Porosity (%)	Thermal conduct (W/mK)
C/C (1#)	Pitch fibers	1.89	6.6	174/164
C/C (2#)	Graphite fibers	1.96	4.0	133/128
C/C (3#)	Graphite fibers	1.94	3.66	119/81
C/C (4#)	–	2.03	3.16	197/190
B_4C–C/C (6#)	7 wt.% B_4C	2.07	3.05	125/122
B_4C–C/C (12#)	10 wt.% B_4C	2.09	3.0	120/118
AEROLOR	Made by France	1.80	–	300/85
CX-20028	Made by Japan	1.74	–	325/186

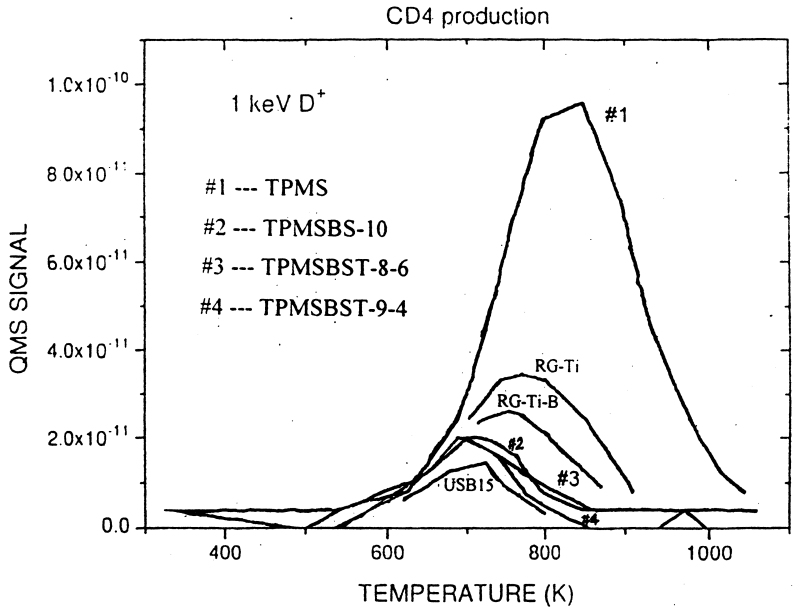

Fig. 5. Chemical sputtering yields of B-, Ti- and Si-doped graphite. RG–Ti, RG–Ti–B and USB15 made by Russia.

perature change relative to the initial state, and S is a factor depending on the geometry and kind of stress. Relative ΔT_c values can serve as a basis for comparison of the performance of different materials under thermal shock stress with fixed geometry. From the energy balance equation, one can obtain the expression of $\Delta T_c = K\Phi t^{1/2}$, where Φ is the energy density (kw/cm^2), t is the pulse length, K is a constant depending only on the physical properties of the materials, except for shear and bending failures for which it can be expected to depend somewhat on the beam diameter. Fig. 7 shows the weight loss of B, Ti, Si-doped graphite with $\Phi t^{1/2}$ by single pulsed laser impingement. Fig. 8 shows the weight loss (total weight lost/irradiation area) of C/C composites with $\Phi t^{1/2}$ by five times pulsed laser impingement. In this figure the experimental result of high purity graphite ISO-880U (made by Japan) is also shown for comparison. A Nd:YAG laser beam with a 0.1-ms pulse length is used in both cases.

4. High heat flux component materials

4.1. SiC, TiC and B_4C coating

SiC, TiC and B_4C coatings on graphite or copper matrix are made by means of Chemical Vapor Deposition (CVD) and Plasma Spraying technique. The thickness of these coatings are 10–1000 μm. The erosion

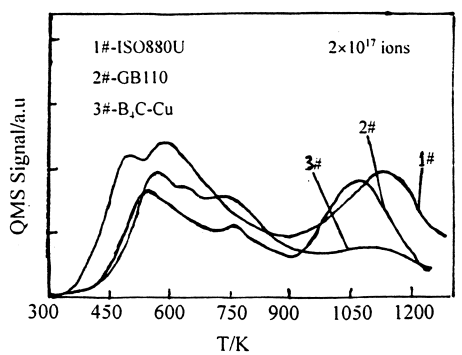

Fig. 6. Thermal desorption spectra of methane for different carbon materials.

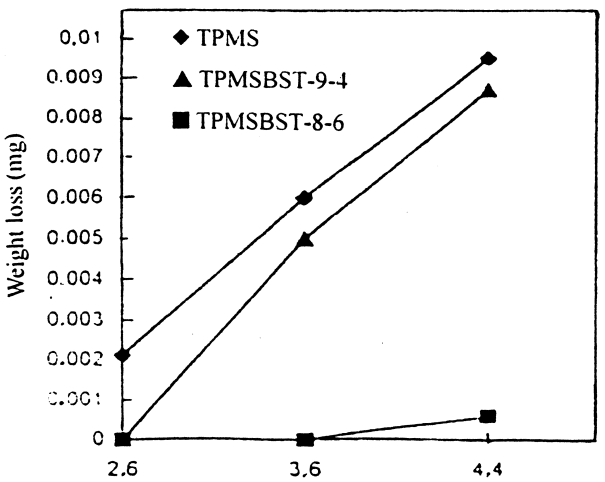

Fig. 7. The weight losses as a function of $\Phi t^{1/2}$ for three kinds of graphite.

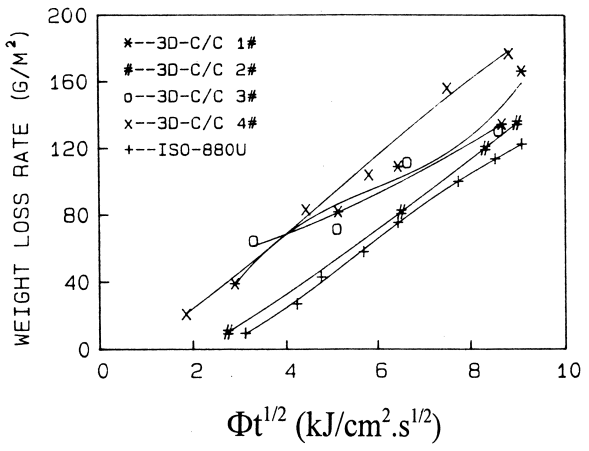

Fig. 8. Weight loss as a function of five laser shots for three-dimesional C/C composites.

experiments of edge plasma are performed both in electron beam thermal shock facility and HL-1M [8,11]. Experimental results show that the cracks occur in the surface of the coating as well as between the coatings and the substrates under a thermal load of 100 MW/m^2 with a 10-ms pulse length. It demonstrates that to strengthen the bonding force between the coatings and substrates is the key issue for the applications of coatings.

4.2. Functionally graded materials (FGM)

In order to strengthen the bonding force between the coatings and substrates and avoid the great mismatch of the thermal expansion coefficient between coatings and substrates, B_4C–C, B_4C–Cu, SiC–C, Mo–Cu and W–Cu functionally graded materials were recently. Chemical sputtering, tritium retention and recycling, and high heat load experiments were carried out. The resistance to thermal shocks of FGM is very significant for coating materials. For example, after shocks of 2-ms electron pulses with 0.5 keV energy and 0.4 A current by 30 times, great cracks, and even fractures, were found not only in the surface but between the surface and the substrate in the B_4C–Cu samples, which were made by plasma spraying immediately (photograph 1S and 1C in Fig. 9), where the thickness of the coating is 160 μm. However, only surface erosions were found in the FGM samples, and almost no cracks occurred on the surface or in the inner layer of the samples (photograph 2S and 2C in

Fig. 9. Thermal load behaviors of B_4C–Cu coating and B_4C–B_4C + Cu–Cu FGM specimen: 1, B_4C coating specimen; 2, FGM specimen; *S*, surface; and *C*, section.

Fig. 9). The thickness of the B_4C surface coating and the graded layer was about 260 μm.

5. Conclusions

In this paper, the two main issues concerning the first wall engineering of tokamak machines are discussed, i.e. the inner wall treating technique by boronization, siliconization and lithium coating, and the plasma facing materials and high heat flux component materials development. After the inner wall conditioning, the hydrogen recycling and the core irradiation energy were lowered, the property of plasma confinement was improved and long pulse discharges were obtained. A series of B, Ti, Si-doped graphite and B_4C–C/C composites were developed, and experimental results indicate that some amounts of B, Ti and Si are helpful in order to restrain chemical sputtering, thus lowering hydrogen retention and recycling, and resisting heat load. Some coating materials, such as SiC, TiC, and B_4C–C or B_4C–Cu coatings materials with graded medium layers were developed. The functionally graded materials, SiC–C, Mo–Cu and W–Cu, were also developed by means of SHS and HIP. Primary experiments indicate FGMs are very promising for plasma-facing materials and high heat flux component applications.

References

[1] F. Waelbroeck, Low-Z materials films in fusion devices, Vacuum 39 (7/8) (1989) 821.
[2] U. Samm, P. Bogen, G. Esser et al., Plasma edge physics with siliconization in TEXOR, J. Nucl. Mater. 220–222 (1995) 25.
[3] J. Winter, Wall conditioning in fusion devices and its influences on plasma performance, Plasma Phys. Contr. Fus. 38 (9) (1996) 1503.
[4] L.L. Peng, E.Y. Wang, N.M. Zhang et al., Improvement of plasma performance with wall conditioning in the HL-1M tokamak, Nucl. Fus. 38 (8) (1998) 1137.
[5] N.M. Zhang, E.Y. Wang, M.X. Wang et al., In situ silicon and lithium coating and its removal in the HL-1M tokamaks, J. Nucl. Mater. 266–269 (1999) 747.
[6] J.P. Qian, F. Zhang, J. Song. Modification of chemical sputtering on B-, Ti- and Si doped graphite, SJSMAES-96, Sapporo, Japan, August 26–28, 1996.
[7] X. Liu, F. Zhang, Z.Y. Xu et al., Thermal desorption behaviors of methane in boron doped graphite, Chin. J. Nucl. Sci. Eng. 19 (1) (1999) 62.
[8] J.P. Qian, X. Liu, P.Y. Li et al., Thermal shock of carbon based materials under high heat flux, J. Nucl. Mater. 191–194 (1992) 340.
[9] Ch. L. You, F. Zhang, M. Ma, et al., A simulated plasma disruption experiment using laser beam. The 3rd SJSMAES'95, Chengdu, 249.
[10] R. Benz, A. Naoumidis, H. Nickel, Thermal shock testing of ceramics with pulsed laser irradiation, J. Nucl. Mater. 150 (1987) 128.
[11] W.Y. Hong, J.P. Qian, et al., Erosion of TiC and SiC coatings in HL-1 Tokamak edge plasma, 4th Sino-Japanese Symp. On MAESFFE, Aug. 26–28, 1996, Sapporo, Japan.